Sigma Journal of Engineering and Natural Sciences
Web page info: https://sigma.yildiz.edu.tr
DOI: 10.14744/sigma.2025.00133

Research Article

Simulations and comparisons of the hay and perez models applied in PVsyst software and their effect on energy output

Sara AL-WAISAWY[1], Hamdiyah S. JASIM[1], Ahmed Hussein DUHIS[1,*]

[1]*Department of Electrical Engineering Techniques, Al-Mussaib Technical College, Al-Furat Al-Awsat Technical University, 54003, Iraq*

ARTICLE INFO

Article history
Received: 12 March 2025
Revised: 08 July 2025
Accepted: 10 July 2025

Keywords:
Horizon Band Irradiation; Photovoltaic System Performance; Solar Radiation Modeling

ABSTRACT

This study examines the connections between essential variables that affect solar energy modeling, such as global horizontal radiation, transposition factor, global incident radiation, energy availability, and horizon band radiation. The PVsyst software evaluates two existing solar radiation models—Hay and Perez—to examine their effects on the energy production of a photovoltaic system in Baghdad City, Iraq. While both models forecast identical global horizontal irradiation, the Perez model yields a superior transposition factor and worldwide incident irradiation owing to its incorporation of horizon band irradiation. The Perez model attains a yearly energy availability of 4792.7 kilowatt-hours, surpassing the Hay model's 4687.2 kilowatt-hours. These findings indicate that incorporating horizon band irradiation markedly enhances the precision of energy yield predictions. The Hay model presents simplicity, whereas the Perez model delivers a more thorough and accurate assessment, especially in scenarios with significant diffuse and near-horizon radiation. This study improved photovoltaic system design by emphasizing the significance of comprehensive solar radiation modeling.

Cite this article as: Al-Waisawy S, Jasim HS, Duhis AH. Simulations and comparisons of the hay and perez models applied in PVsyst software and their effect on energy output. Sigma J Eng Nat Sci 2025;43(5):1–12.

INTRODUCTION

Output compute models are employed to assess the anticipated energy output for a photovoltaic system, requiring specific input parameters, including global sun irradiation. Given that minor uncertainty in model parameters can cause significant discrepancies in anticipated investment returns, it is imperative to minimize uncertainties arising from model inputs to the greatest extent possible.

Estimating sun radiation on tilted surfaces with varying orientations is crucial for calculating the electrical power produced by photovoltaic systems, designing solar energy systems, and assessing their long-term performance average [1, 2]. Nonetheless, the existing measurement data are inadequate, as global horizontal and diffuse horizontal radiation readings from pyrometers are sometimes the sole available data in numerous places. Nevertheless, inclined measurements are implemented. The selected tilt angle may not be advantageous for the specific site.

Therefore, the solar radiation received on a slanted surface must be calculated by converting solar radiation from a

***Corresponding author.**
*E-mail address: ah.hu.khf@gmail.com

This paper was recommended for publication in revised form by Editor-in-Chief Ahmet Selim Dalkilic

Published by Yıldız Technical University Press, İstanbul, Turkey

level surface to the radiation incident on the specified tilted surface [3-6].

Transposition models that use global and scattered horizontal sunlight have been commonly used within the solar energy field to calculate the sunlight hitting tilted solar panels. Transposition models break down the sunlight on a tilted surface into three parts: direct, diffuse, and sunlight mirrored from the ground. Direct radiation can be calculated by determining the geometry between horizontal and tilted surfaces. The ground reflected radiance can be calculated with the assistance of an isotropic model utilizing simple algorithms. The idea that everything is the same in all directions can work for figuring out how opacity affects things, but it's not as useful for the scattered light part. This is because the way the diffuse light spreads out is complicated and relies on several things, like the angle of the sun and the presence of clouds. The ongoing development and variety of transposition models demonstrate the intricacy of the task.[7-9]

Initial models transformed horizontal diffuse radiation to a tilted plane by presuming that total sky diffuse radiation is isotopically distributed across the sky dome [10-14]. This idea is overly simplistic and does not align with reality. Recent transposition models consider the diffuse component to be anisotropically distributed. Some anisotropic models solely account for an isotropic backdrop and an extra circumsolar region, while others also incorporate horizon-brightening effects. This assumption holds only when clouds are absent, as overcast conditions result in a darker horizon than the zenith [15, 16]. Solar Energy is a renewable, safe, and abundant energy source. Calculating the amount of solar radiation incident upon inclined surfaces with different orientations is required to calculate the building envelope's heat gain and the power generated by photovoltaics [17, 18], design solar systems, and evaluate their long-term average performance. Given the reality that several meteorological/radiometric sites measure global as well as diffuse irradiation on horizontal surfaces, data for inclined surfaces are not accessible. They are calculated using different models than those measured upon horizontal surfaces [19-21].

The total radiation incident on a tilted surface comprises beam, diffuse, and ground reflection. Hourly, straightforward algorithms can accurately compute the direct and reflect components, but the diffused component is more complex, necessitating review and appraisal of the necessary procedures.[22, 23].

Several of these evaluations have focused on computational methods for modeling and evaluating the performance of solar systems. In this context, Connolly et al. [24] provided a comprehensive overview of current computational techniques for assessing the integration of renewable energy initiatives. Several software programs are widely utilized as the foundation for several scientific projects. Wijeratne et al. [25] thoroughly assessed the software tools employed in several research for the simulation of photovoltaic systems. The efficacy of these PV techniques unequivocally influences the quality of the outcomes achieved in the studies above. Nevertheless, limited research has evaluated the effectiveness of various existing photovoltaic simulation software tools compared to actual photovoltaic system energy output data.

Lee et al. [26] validated four photovoltaic tools (PVsyst, HOMER, and SAM) using actual production data collected from six photovoltaic systems located at the Desert Knowledge the Country Solar Centre, a solar technology demonstration facility situated in Alice Springs, Australia. The systems comprised modules utilizing various photovoltaic technologies: monocrystalline, polycrystalline, amorphous silicon, and cadmium telluride thin-film modules. The installed capacity of the photovoltaic arrays varied from 5.1 kW to 7 kW. The modeling tools demonstrated accuracy, with annual average percentage discrepancies ranging from −1.44% to −4.93%, contingent upon the installation type. HOMER and RETScreen yielded the most precise results, but PVsyst typically produced conservative outcomes. Despite being the most straightforward of the models, Sunny yielded the least precise outcomes.

Axaopoulos et al. [27] evaluated the efficacy of six software tools (TRNSYS, Archelios, Polysun, PVSyst, PV*SOL, and PVGIS) utilizing the actual electrical energy produced by a grid-connected 19.8 kWp solar system situated in Thrace, Greece. Their findings indicated that all instruments generally overestimated the global irradiance received by the photovoltaic modules while dramatically underestimating the electrical energy produced by the system. The tool that demonstrated the most superior overall performance was TRNSYS, followed by Archelios. The findings indicated that software-reliant on a PVGIS irradiation database may exhibit considerable inaccuracies, particularly when analyses are conducted for specific months or brief timeframes.

Freeman et al. [28] evaluated four prominent solar modeling tools (SAM, PVWatts, PVsyst, and PV*SOL Expert) using actual data from nine photovoltaic systems comprising three utility-scale systems and six commercial-scale systems. In this study, they broadened the findings of prior research [29, 30] that solely assessed the SAM tool. The yearly results for the tools exhibited relative errors ranging from 1.4% to -16.2%. In this instance, PVWatts appeared as an anomaly among the nine systems. Excluding the outliers, overall annual errors fell within 8%. On the hourly scale, excluding two particular outliers, all root mean square errors (RMSE) remained below 7% for all tools and systems. This study presented disaggregated errors for various PV systems, rendering it impossible to determine which tool was superior.

De Souza Silva et al. [31] recently performed a comparison analysis of various photovoltaic power simulation software packages (PVsyst, PV*SOL, and HOMER) utilizing production data from the 336.96 kWp photovoltaic plant at the Campinas University (Brazil). The findings indicated that PV*SOL yielded more conservative outcomes, whilst HOMER produced the most optimistic results. Based on the annual discrepancies between the software tools' outputs and the actual values of the PV plant, PVsyst demonstrated superior performance, with an error rate of 1.02%. In comparison, HOMER was followed by an error of 2.04%. PV*SOL had a greater, albeit more cautious, error of −10.38%.

Converting solar radiation measurements from a horizontal to a tilted surface (and vice versa) is a typical difficulty in solar energy system design. Many models deal with this problem; the first findings date back to [23], which presuppose an isotropic in the sky hemisphere. However, this anisotropic aspect of diffuse irradiance has been a well-known source of inaccuracy associated with that assumption [32-34]. To address this issue, various anisotropic models have been proposed [35-38]. [39, 40] have identified a Perez model (Perez et al., 1990, 1988, 1987, 1986) [41-44] as the most popular and ubiquitous transposition model (for all locations). The Perez model has been employed in numerous studies for various applications. For instance, [45] optimized PV array outputs by modifying the orientation and tilt of the array, while [46] employed the model to analyze building-integrated photovoltaic systems.

Figure 1 shows that the diffuse part of global solar radiation comprises the circumsolar-diffused part, isotropic diffuse radiation from the sky, diffuse irradiation from the horizon, and radiation reflected off the ground (albedo).

To calculate the irradiation on a tilted plane, the two models presented in this analysis consider distinct components that comprise the diffuse radiation.

In 1979, Hay [35] introduced a model to calculate the scattered portion of the radiation on inclined surfaces based on the radiation data obtained on a horizontal surface. The model posits the concept of the transposition factor has two distinct parts. One of the models takes into account the isotropic background. In contrast, the other model includes a circumsolar component that varies in inverse proportion to the zenith angle (θz) as well as the angle of incidence of the direct irradiation (θi). Hay has established an index, which is assigned to every component that is considered in the model.

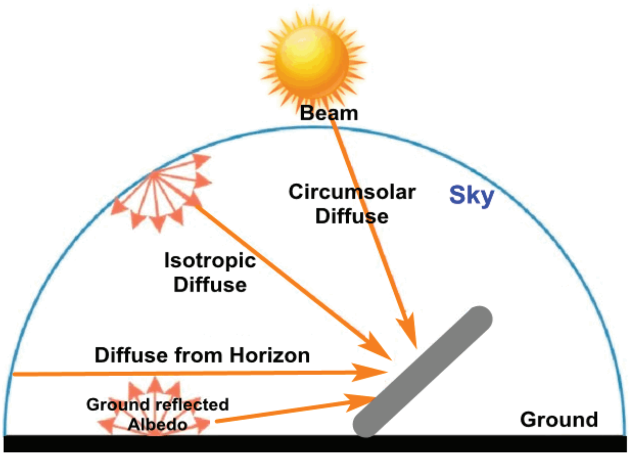

Figure 1. Diffuse component of the global solar radiation.

The index is determined by dividing the direct irradiation incident on the horizontal axis (HBI) by the extraterrestrial irradiance (I_o). This factor is designed to convert the impact of the atmosphere on the scattered sunlight, resulting in a decrease in interference on days with clear skies. As a result, the index typically approaches a value of 1. Therefore, the circumsolar component is more critical, as demonstrated in equation (1).

$$TDI = HDI\left[\left(\frac{HBI}{I_o}\right)\frac{\cos\theta_i}{\cos\theta_z} + \left(1 - \frac{HBI}{I_o}\right)\frac{1+\cos\beta}{2}\right] \quad (1)$$

Where *HID* is horizontal diffuse Irradiation, TDI is tilted surface diffuse irradiation, and b indicates the solar panels' inclination angle regarding the ground.

Despite its widespread use in simulation software for solar systems, Hay's model lacks consideration for a critical component termed the horizon, which significantly contributes to the quantity of diffuse radiation on an inclined plane. Thus, Perez's model incorporated the impact of the horizon within the model [11]. Furthermore, the previous models created by Perez failed to consider some scenarios, such as the amplification of circumsolar components in atmospheres with a high fraction of diffuse radiation combined with extreme brightness [47].

The suggested model can be utilized for a broader range of celestial arrangements, in which the horizon and circumsolar elements that intersect with the isotropic dome are assigned specific weights represented by its coefficients *F*1 and *F*2, respectively. The coefficients fluctuate based on the degree of clarity, brightness index, and empirical coefficients [44].

In 1987, Perez introduced a revised and streamlined version in which the coefficients. F'_1 and F'_2 Were redefined. The component *F*2 can have negative values, indicating the trade-off between the radiance of the horizon and the brightness directly overhead. The phenomenon of horizon brightness is typically observed on days with clear skies, while the zenith component is observed on foggy days [43]. In 1990, modifications were implemented to ensure that the clarity index is not influenced by the angle of the zenith [41].

The finalized version of the model quantifies the scattered radiation on the inclined surface using equation (2).

$$TDI = HDI\left[\left((1-F_1')\right)\left(\frac{1+\cos\beta}{2} + F_1'(a/b) + F_2'\sin\beta\right)\right] \quad (2)$$

Where a and b are a = max (0, cosθ) , b= max (0.087, cosΦ), F'_1 and F'_2 are horizon/zenith and circumsolar

The PV syst. software includes two transposition modules, Hay and Perez, which calculate the global irradiation incidence on the collector plane (GlobInc) based on the global horizontal irradiation (GlobHor).

The transposition factor (TF) quantifies the correlation between the global radiation on the tilted plane (TDI) and the global irradiation on a horizontal plane HBI [39]. In simulation, the term "GlobInc" is the equivalent of " TDI " in theoretical terms, whereas "GlobHor" is the equivalent of " HBI ". The metric that carries more significance in computing the transposition factor (TF) is the (GlobInc), as the (GlobHor) remains constant at all locations.

No authors have utilized the Perez and Hay models through simulation with PV Syst software to analyze the impact of each model on the TF, GlobInc, and energy production in a solar system in Baghdad city . Simulations for two models were conducted with the same system power of 2840 Wp.

The paper structure follows design methodology in Section 2, results, and discussion in Section 3. Finally, the conclusions of the study are presented in Section 4.

MATERIALS AND METHODS

The PV Syst software includes two transposition modules (Hay and Perez) that are used to calculate the (GlobInc) from (GlobHor). The following five steps in the sequence are necessary for simulating PVSyst.

Step 1: Selection of the Site

The PVSYST has the advantage that the software developer automatically links the latitude and longitude data acquired from the NASA-SSE satellite station following the installation site choice.

The site where a PV-based power plant has to be built is quite essential, as it needs to be connected to a data source, and such software requires NASA-SSE satellite data. The place of system implementation was Baghdad. The particular geographical position of Baghdad is depicted in table (1). The meteorological data that was obtained from the NASA website for the location is shown in table (2)

Where DiffHor is Horizontal diffuse irradiation

Step 2: Fixing the Azimuth and Tilt angles

As shown in Figure 2, the tilt angle of 31° is considered the optimal value for achieving maximum irradiance and zero losses concerning optimum. Furthermore, the azimuth angle is set at 0o due to the same rationale.

Step 3: Daily Consumptions

Table 3 presents the energy usage and load data of a small residence. According to the data in this table, the daily energy usage amounts to 8427 Wh, while the overall power demand is 5.995 kW.

Step 4: System Definitions

Once the location's orientation, latitude and longitude, solar radiation statistics, and electricity demand have been collected, the system can be developed, modeled, and simulated. The design and modeling processes cannot begin without first determining the components that will be used. The standalone PV system configuration is shown in figure (4). The main component characteristics necessary for the design of a standalone PV system are shown in table 4

Step 5: Choosing the Transposition Mode

The Hay and Perez models are the two transposition models available to PVsyst. for modeling irradiation. In

Table 1. Geographical location data of Baghdad City

Site	Country	Region	Latitude	Longitude	Altitude	Time Zone	Albedo
Baghdad	Iraq	Asia	33.3406°	44.4009°	45m	3GMT	0.2

Table 2. Baghdad meteorological data obtained from the NASA website

Month	GlobH	DiffHor	Values	GlobH	DiffH
	kWh/m²	kWh/m²	Month	kWh/m²	kWh/m²
January	91.8	28.5	July	217	63.9
February	112.8	30.8	August	208	53.6
March	154.4	46.2	September	166.5	45.6
April	161.7	60.6	October	123.4	41.2
May	200.9	67	November	89.4	31.2
June	226.8	58.8	December	81.2	27.3
Year				1833.9	554.7

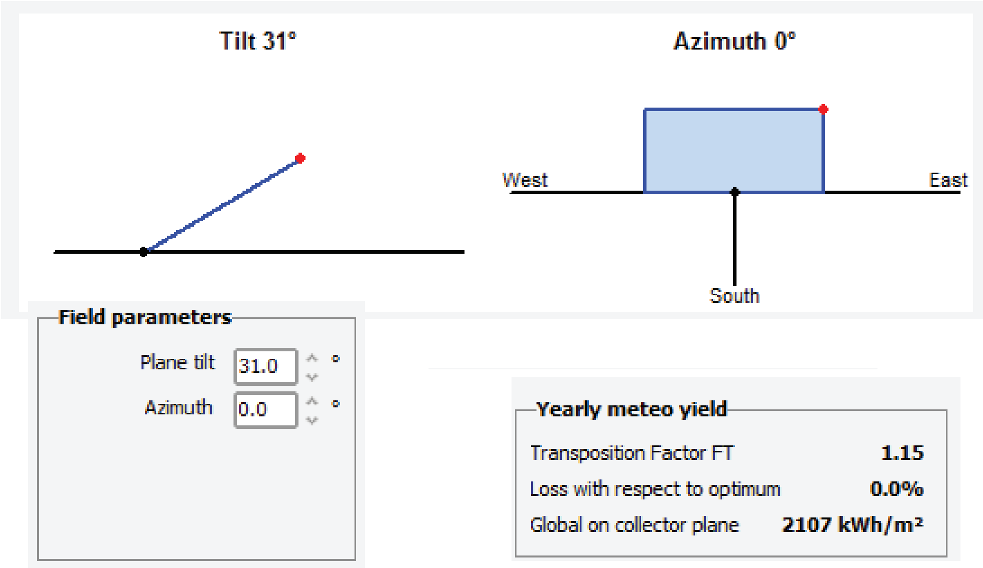

Figure 2. Azimuth and Tilt angles of PV system.

Table 3. The daily consumption of energy for the site

Number	Appliance	Power	Use	Energy
		W	Hour/day	Wh/day
8	Lamps (LED or fluo)	9W/lamp	7	504
1	TV	80W/app	5	400
3	Fan	65W/app	8	1560
2	Fridge / Deep-freeze	2.5 KWh/day	12	4999
1	Dish- and Cloth-washer	250 W aver.	2	500
1	Laptop	80W/app	4	320
Stand-by consumers		6 W lot	24	144
Total daily Energy				8427Wh/day
Monthly Energy				252.8 KWh/mth

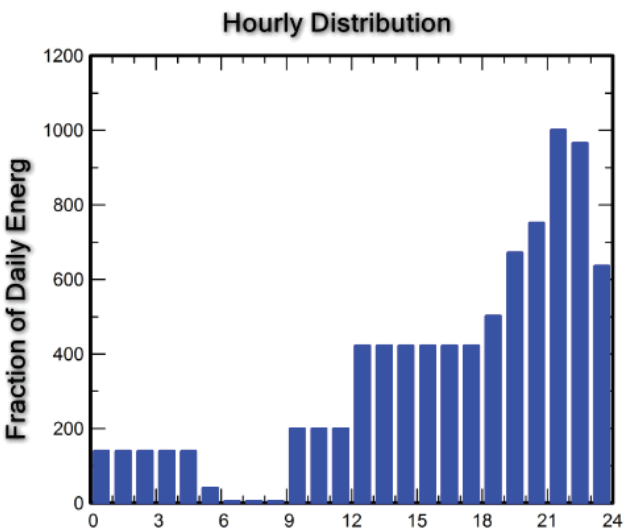

Figure 3. The daily consumption energy for the site.

PVsyst, the Perez 1990 model is the default transposition model used. Selecting a transposition model based on the PV Syst software settings is possible. In this study, two different cases will be compared to determine the TF. Case 1 uses the Hay model, and case 2 uses the Perez model

RESULTS AND DISCUSSION

The study's site is at a longitude of 44.4009°, a latitude of 33.3406°, and an elevation of 45m meters. Data on global irradiation incidents on a horizontal plane is obtained from the NASA meteorology and solar energy website and entered into the PVSyst. Meteorological directory as shown in table (1). The simulation will be for Standalone system with batteries with a system power of 2840 Wp

Two simulations utilizing PV Syst software were conducted employing the Perez and Hay transposition model to compute the irradiance on the plane of the array based

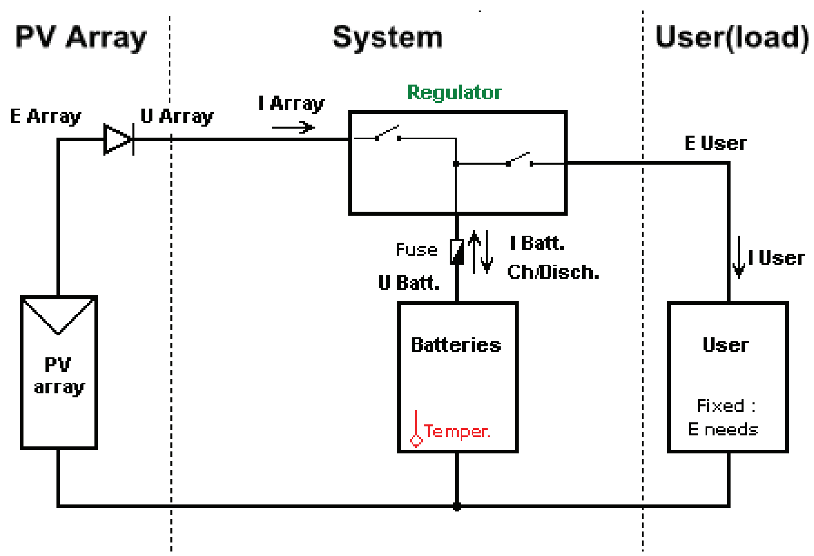

Figure 4. Standalone PV system configuration.

Table 4. illustrates the main component characteristics necessary for the design of a standalone PV system

PV module		**Battery**	
Manufacturer	LG Electronics	Manufacturer	Electrona
Model	LG 355 N1K-N6	Model	6B50 - Starting
(Original PVsyst database)		Technology	Lead-acid, sealed
Unit Nom. Power	355 Wp	Nb. of units	10 in parallel x 4
Number of PV modules	8 units	Discharging min. SOC	20.0 %
Nominal (STC)	2840	Stored Energy	16.9 Kwh
Modules	4 Strings x 2 In series		
At operating cond. (50°C)		**Battery Pack Characteristics**	
Pmpp	2605 Wp	Voltage	48 V
U mpp	62V	Nominal Capacity	440 Ah (C10)
I mpp	42A	Temperature	Fixed 20°C
Controller		**Total PV Power**	
Universal controller		Nominal (STC)	3 Kwp
Technology	MPPT converter	Total	8 modules
Temp coeff.	-5.0 mV/°C/Elem.	Module area	14.7 m^2

on the monthly and yearly measurements of GlobInc, given that GlobHor remains constant at the exact location. The comparison will assess TF by utilizing each model to see which model influences the output of E_Avail energy.

Case 1: Hay Model

Select the Hay Model in the PV Syst software from the project settings. The simulation results for this case study about the main components of global irradiation are presented in Table 5.

As seen in Table 5, GlobInc is the sum of Beam incident on the collector plane (BeamInc), circumsolar incident on the collector plane (CircInc), sky diffuse incident on the collector plane (DifSInc), and albedo incident on the collector plane (Alb_Inc). At the same time, the horizon band in the vertical plane (HBndVrt) is 0 kWh/m^2.

The yearly and monthly main essential results, as shown in table (6)

From table (6), the effective global radiation in the collection plane (GlobEff) is 1957.3 kWh/m^2. The system will

Table 5. Main components of the global irradiation for case 1

	GlobInc	BeamInc	CircInc	DifSInc	Alb_Inc	HBndVrt
	kWh/m²	kWh/m²	kWh/m²	kWh/m²	kWh/m²	kWh/m²
January	132.2	83	18.06	29.82	1.31	0
February	151.9	104.7	20.05	25.53	1.612	0
March	180.2	119.9	21.92	36.2	2.205	0
April	164.1	99.3	18.99	43.42	2.309	0
May	186.1	115.4	20.94	46.85	2.869	0
June	200.2	142.4	21.76	32.78	3.239	0
July	196.5	134.5	22.01	36.87	3.099	0
August	204.6	140.4	23.63	37.58	2.971	0
September	186.2	130.4	22.02	31.36	2.378	0
October	150.9	87.1	19.98	42.08	1.762	0
November	124.2	75.5	16	31.48	1.277	0
December	124	80.5	16.78	25.6	1.16	0
Year	2001.1	1313.2	242.16	419.56	26.193	0

Table 6. Annual and monthly main significant results for case 1

	GlobHor	GlobInc	TF	GlobEff	E_Avail
	kWh/m²	kWh/m²	ratio	kWh/m²	kWh
January	91.8	132.2	1.441	130	332.7
February	112.8	151.9	1.346	149.3	377.5
March	154.4	180.2	1.167	176.8	438.1
April	161.7	164.1	1.015	160.2	385
May	200.9	186.1	0.926	181.2	426.4
June	226.8	200.2	0.883	194.9	449.4
July	217	196.5	0.906	191.4	436.5
August	208	204.6	0.983	199.7	455.9
September	166.5	186.2	1.118	182.3	420.3
October	123.4	150.9	1.223	147.9	355.4
November	89.4	124.2	1.389	121.9	301.5
December	81.2	124	1.527	121.8	308.5
Year	1833.9	2001.1	1.091	1957.3	4687.2

produce an annual energy output of 4687.2 kWh; when dividing GlobInc by GlobHor, the resulting ratio is the transposition factor (TF)

Case 2: Perez Model

Select the Perez Model from the project settings in the PV Syst software. The simulation results for this case study about the main components of global irradiation are presented in Table 7.

As shown in table (8), yearly and monthly main significant results

From table (8), the effective global radiation in the collection plane (GlobEff) is 2003.9 kWh/m². The system will produce an annual energy output of 4792.7kWh when dividing GlobInc by GlobHor; the resulting ratio is the transposition factor (TF)

The outcomes show that the significant factors influencing solar power model predictions the (TF), (E_Avail (GlobHor), (HBndVrt), and Global Incident Irradiation (GlobInc)—are inherently interdependent. The efficacy as well as of a solar power system is determined by the cumulative effects of each parameter on the others.

Table 7. Main components of the global irradiation for case 2

	GlobInc	BeamInc	CircInc	DifSInc	Alb_Inc	HBndVrt
	kWh/m²	kWh/m²	kWh/m²	kWh/m²	kWh/m²	kWh/m²
January	135.7	83	22.46	28.89	1.31	2.856
February	155.2	104.7	22.87	25.97	1.612	4.427
March	184.8	119.9	28.88	33.79	2.205	5.665
April	167.9	99.3	28.75	37.5	2.309	5.226
May	189.9	115.4	32.02	39.6	2.869	6.941
June	204.3	142.4	27.88	30.73	3.239	8.035
July	200.7	134.5	30.33	32.71	3.099	8.056
August	209	140.4	31.11	34.58	2.971	7.397
September	190.3	130.4	27.1	30.43	2.378	6.152
October	155.5	87.1	28.5	38.11	1.762	3.752
November	127.3	75.5	20.64	29.93	1.277	2.375
December	126.7	80.5	19.53	25.47	1.16	2.667
Year	2047.2	1313.2	320.07	387.71	26.193	63.551

Table 8. Annual and monthly main important results for case 2

	GlobHor	GlobInc	TF	GlobEff	E_Avail
	kWh/m²	kWh/m²	ratio	kWh/m²	kWh
January	91.8	135.7	1.479	133.4	341.5
February	112.8	155.2	1.375	152.5	385.2
March	154.4	184.8	1.197	181.3	448.6
April	161.7	167.9	1.038	164.2	393.7
May	200.9	189.9	0.945	185.2	435
June	226.8	204.3	0.901	199	458.2
July	217	200.7	0.925	195.6	445.5
August	208	209	1.005	204.2	465.5
September	166.5	190.3	1.143	186.4	429.1
October	123.4	155.5	1.26	152.5	366
November	89.4	127.3	1.424	125	309.3
December	81.2	126.7	1.559	124.4	315.2
Year	1833.9	2047.2	1.116	2003.9	4792.7

Baseline solar irradiance on a horizontal plane is represented by GlobHor, while solar radiation collected on the tilted collector plane is defined by GlobInc.

HBndVrt, as a component of the Perez model, consistently exhibits more GlobInc than the Hay model. In the Perez model, GlobHor and GlobInc possess 1833.9 kWh/m² and 2047 kWh/m², respectively. GlobHor measures 1833.9 kWh/m² compared to the Hay model, while GlobInc measures 2001 kWh/m².

As a result of HBndVrt direct addition to the GlobInc for the Perez model, both TF and E_Avail are increased. Reduced GlobInc and somewhat diminished system performance are the outcomes of HBndVrt's exclusion from the Hay model. In the Perez model, GlobInc is 126.7 kWh/m² in December, while HBndVrt is 2.667 kWh/m². Contrasted with GlobInc 124 kWh/m², HBndVrt is 0 kWh/m².

An increase in GlobInc leads to an increase in TF, improving the irradiation that may be used to produce energy. When HBndVrt is included in the Perez model, the TF is marginally greater than in the Hay model. Annual TF in Hay is 1.091, while in Perez, it is 1.116.

As shown in figure (5), the GlobHor, GlobInc, and TF for Perez and Hay models

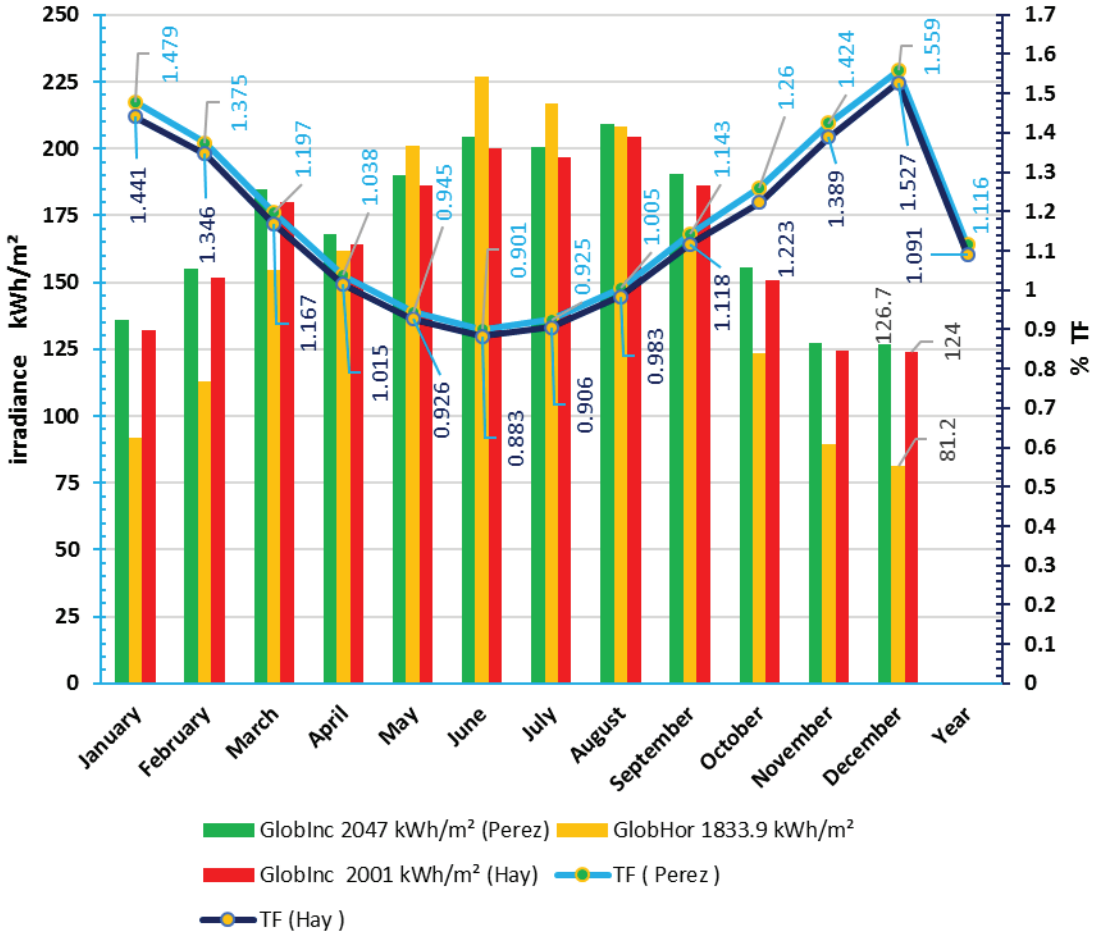

Figure 5. The monthly and yearly of GlobHor, GlobInc, and TF for Perez and Hay models.

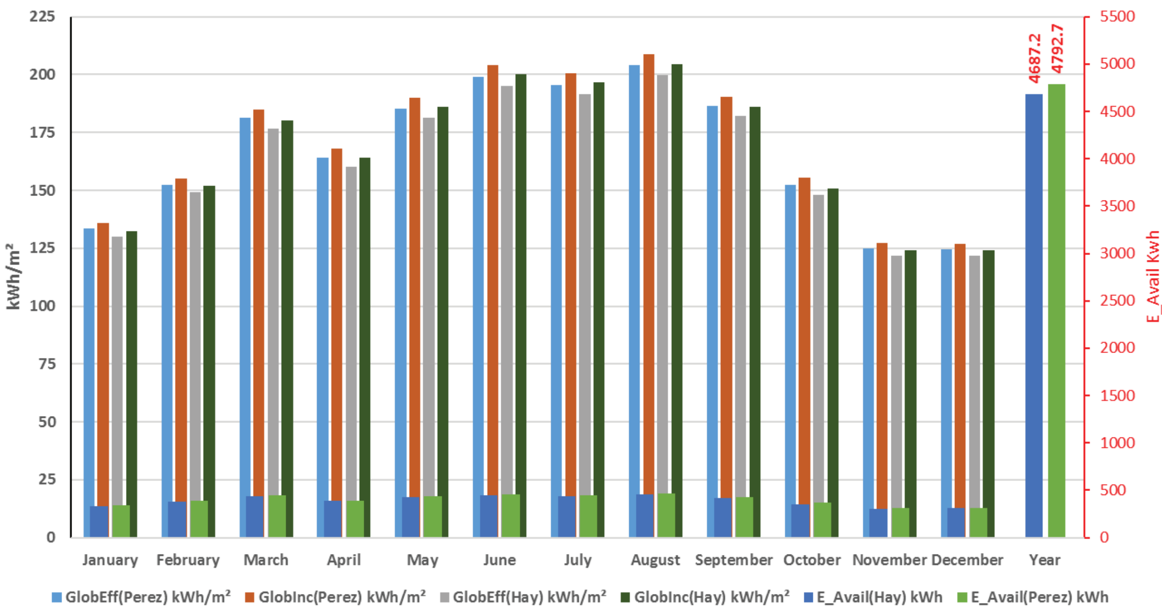

Figure 6. The monthly GlobEff and GlobInc concerning E_Avail yearly for Perez and Hay models.

Figure 6 shows the effect of increasing GlobInc, GlobEff on increasing E_Avail in the Perez model compared with the Hay model

For January, Perez had TF is1.479 and GlobInc is 135.7 kWh/m², whereas Hay's model E_Avail was directly reliant on GlobInc with TFis1.441 and GlobInc Equal 132.2 kWh/m². If all other system parameters stay the same, an increase in GlobInc will increase E_Avail.

E_Avail is marginally more in the Perez model than in the Hay model because of the larger GlobInc caused by HBndVrt.

Perez model gives an annual E_Avail of 4,792.7 kWh. While the Hay model is 4687.2 kWh.

During the winter months, such as January and December, the higher TF compensates to the lower GlobHor, thereby maintaining an acceptable GlobInc as well as E_Avail.

These months, GlobInc experiences a discernible influence from HBndVrt. In December, the Perez model had GlobHor is 81.2 kWh/m², TF is 1.559, HBndVrt is 2.667 kWh/m², GlobInc is 126.7 kWh/m², and E_Avail is 315.2 kWh, while the Hay model had GlobHor is 81.2 kWh/m², TF is 1.527, HBndVrt is 0 kWh/m², GlobInc is 124 kWh/m², and E_Avail is 308.5 kWh.

In summer months, such as June and July, the TF experiences a slight decrease due to the increased solar angles. However, the GlobHor increases considerably, ensuring that the GlobInc and E_Avail remain high. For instance, in June, the Perez model yielded GlobHor is 226.8 kWh/m², TF is 0.901, HBndVrt is 8.035 kWh/m², GlobInc is 204.3 kWh/m², and E_Avail is 458.2 kWh, while the other model yielded GlobHor is 226.8 kWh/m², TF is 0.883, HBndVrt is 0 kWh/m², GlobInc is 200.2 kWh/m², and E_Avail is 449.4 kWh. Within the Hay paradigm

CONCLUSION

This study analyzes the impact on essential solar performance metrics, such as TF, GlobInc, and E_Avail, assessed on a monthly and annual basis. The findings indicate that incorporating the horizon band component (HBndVrt) into the Perez model enhances transposition accuracy and produces higher energy yield estimates when compared to the more straightforward Hay model.

The Perez model more effectively predicts sunlight conditions in Baghdad, where haze and dust are common, by providing a more accurate representation of scattered light and the horizon. This underscores the significance of choosing a transposition model that accurately represents the local climate in the design or simulation of photovoltaic systems.

Monthly data reveal how TF compensates for seasonal changes in solar angles, especially in winter months, maintaining energy availability even when GlobHor is reduced. Annual results further emphasize the Perez model's effectiveness, with a higher TF (1.116 vs. 1.091) and annual energy availability (4792.7 kWh vs. lower values from Hay). These metrics are critical for accurate long-term performance assessments and system sizing.

Ultimately, this study underscores the significance of using more comprehensive sky models, like Perez, to optimize the design and prediction accuracy of solar energy systems, particularly in regions with variable diffuse radiation. The findings reinforce the value of both monthly and annual analysis scales in ensuring robust, context-sensitive solar energy planning.

AUTHORSHIP CONTRIBUTIONS

Authors equally contributed to this work.

DATA AVAILABILITY STATEMENT

The authors confirm that the data that supports the findings of this study are available within the article. Raw data that support the finding of this study are available from the corresponding author, upon reasonable request.

CONFLICT OF INTEREST

The author declared no potential conflicts of interest with respect to the research, authorship, and/or publication of this article.

ETHICS

There are no ethical issues with the publication of this manuscript.

STATEMENT ON THE USE OF ARTIFICIAL INTELLIGENCE

Artificial intelligence was not used in the preparation of the article.

REFERENCES

[1] Mehleri ED, Zervas PL, Sarimveis H, Palyvos JA, Markatos NC. A new neural network model for evaluating the performance of various hourly slope irradiation models: implementation for the region of Athens. Renewable Energy 2010;35:1357–1362. [CrossRef]

[2] Arun S, Nagoorvali SK, Kumar KS, Mohan GS. Automation of main bearing bolt and cap loosening machine for automobile crankshaft. Int J Mech Eng Technol 2017;8:41–49.

[3] Allw AS, Duhis AH, Al-Ghanimi A. An efficient of estimation the load profile analysis of photovoltaic system with different shading of local city. Int J Power Electron Drive Syst 2022;13:2405–2413. [CrossRef]

[4] Kudish AI, Evseev EG. Prediction of solar global radiation on a surface tilted to the south. SPIE 7046:9–20. [CrossRef]
[5] Güven AF, Yörükeren N. A comparative study on hybrid GA-PSO performance for stand-alone hybrid energy systems optimization. Sigma J Eng Nat Sci 2024;42:1410–1438. [CrossRef]
[6] Awogbemi O, Von Kallon DV, Kumar KS. Contributions of artificial intelligence and digitization in achieving clean and affordable energy. Intell Syst Appl 2024;200389. [CrossRef]
[7] Riechelmann S, Schrempf M, Seckmeyer G. Simultaneous measurement of spectral sky radiance by a non-scanning multidirectional spectroradiometer (MUDIS). Meas Sci Technol 2013;24:125501. [CrossRef]
[8] Mutlu B, Özyörük B. A research on mathematical model approaches in biomass supply chain. Sigma J Eng Nat Sci 2024;42:945–955. [CrossRef]
[9] Kumar KS, Raju DBN, Arulmani J, Amirthalingam P. Design and structural analysis of liquified cryogenic tank under seismic and operating loading. Int J Mech Eng Technol 2016;7:345–366.
[10] Klein SA. Calculation of monthly average insolation on tilted surfaces. Solar Energy 1977;19:325–329. [CrossRef]
[11] Duffie JA, Beckman WA, Blair N. Solar engineering of thermal processes, photovoltaics and wind. Hoboken: John Wiley & Sons; 2020.
[12] Badescu V. 3D isotropic approximation for solar diffuse irradiance on tilted surfaces. Renewable Energy 2002;26:221–233. [CrossRef]
[13] Javanjal VK, Patil LN, Mahajan KA, Patil AA. Examining the role of nano-sized additives in boosting air conditioner efficiency. Sigma J Eng Nat Sci 2025;43:107–120. [CrossRef]
[14] Kumar KS, Muniamuthu S, Tharanisrisakthi BT. An investigation to estimate the maximum yielding capability of power for mini venturi wind turbine. Ecol Eng Environ Technol 2022;23. [CrossRef]
[15] Grant RH, Heisler GM. Obscured overcast sky radiance distributions for ultraviolet and photosynthetically active radiation. J Appl Meteorol Climatol 1997;36:1336–1345. [CrossRef]
[16] Kumar S, Gaur A, Kamal N, Pathak M, Shrinivas K, Singh P. Artificial neural network based optimum scheduling and management of forecasting municipal solid waste generation–case study: Greater Noida in Uttar Pradesh (India). IOP Conf Ser Mater Sci Eng 1478:012033. [CrossRef]
[17] Cheng CL, Chan CY, Chen CL. An empirical approach to estimating monthly radiation on south-facing tilted planes for building application. Energy 2006;31:2940–2957. [CrossRef]
[18] Kumar S, Sharma SS, Giri J, Makki E, Sathish T, Panchal H. Perovskite materials with improved stability and environmental friendliness for photovoltaics. Front Mech Eng 2024;10:1357087. [CrossRef]
[19] Burlon R, Bivona S, Leone C. Instantaneous hourly and daily radiation on tilted surfaces. Solar Energy 1991;47:83–89. [CrossRef]
[20] Aljanabi M, Al-Kafaji MSS, Duhis AH. Optimum yearly and seasonal tilt angle of solar system in the center of Babylon/Iraq using PVsyst software. Indones J Electr Eng Comput Sci 2023;31:626–635. [CrossRef]
[21] Kumar S, Dave V. Backpropagation algorithm-based approach to mitigate soiling from PV module. In: Intelligent Computing Techniques for Smart Energy Systems: Proceedings of ICTSES 2018. Singapore: Springer; 2019. p. 153–161. [CrossRef]
[22] Duhis AH, Mosheer AD, Abed AM. Optimization of seasonal tilt adjustment photovoltaic system in Karbala, Iraq, by using the albedo benefit. Indones J Electr Eng Comput Sci 2023;32:632–642. [CrossRef]
[23] Bishnoi D. Pressure exertion and heat dissipation analysis on uncoated and ceramic (Al2O3, TiO2 and ZrO2) coated braking pads. Mater Today Proc 2023;74:774–787. [CrossRef]
[24] Connolly D, Lund H, Mathiesen BV, Leahy M. A review of computer tools for analysing the integration of renewable energy into various energy systems. Appl Energy 2010;87:1059–1082. [CrossRef]
[25] Wijeratne WMPU, Yang RJ, Too E, Wakefield R. Design and development of distributed solar PV systems: do the current tools work? Sustain Cities Soc 2019;45:553–578. [CrossRef]
[26] Lee GR, Frearson L, Rodden P. An assessment of photovoltaic modelling software using real world performance data. CCH Hamburg, Germany: 4339–4343.
[27] Axaopoulos PJ, Fylladitakis ED, Gkarakis K. Accuracy analysis of software for the estimation and planning of photovoltaic installations. Int J Energy Environ Eng 2014;5:1–7. [CrossRef]
[28] Freeman J, Whitmore J, Blair N, Dobos AP. Validation of multiple tools for flat plate photovoltaic modeling against measured data. IEEE:1932–1937.
[29] Freeman J, Whitmore J, Kaffine L, Blair N, Dobos AP. System advisor model: flat plate photovoltaic performance modeling validation report. Golden (CO): National Renewable Energy Lab (NREL); 2013. [CrossRef]
[30] Soni P, Dave V, Kumar S, Paliwal H. A comparative study of AI-driven techno-economic analysis for grid-tied solar PV-fuel cell hybrid power systems. Sci Temper 2024;15:2248-2257. [CrossRef]
[31] de Souza Silva JL, Costa TS, de Melo KB, Sakô EY, Moreira HS, Villalva MG. A comparative performance of PV power simulation software with an installed PV plant. IEEE:531–535. [CrossRef]
[32] Ma CCY, Iqbal M. Statistical comparison of models for estimating solar radiation on inclined surfaces. Solar Energy 1983;31:313–317. [CrossRef]

[33] Kumar S, Supriya J, Sharma SS, Paliwal H, Manikanta G, Giri J, et al. Developments, challenges, and projections in solar battery charging in India. Results Eng 2024;103248. [CrossRef]
[34] Thirunavukkarasu M, Sujit K, Ramadass S, Manihoman MP, Elahi Mohammad SM, Rezaul KM, et al. Feature of SiO2 concentration on solar thermal functional characteristics of flat plate solar collector. Therm Sci 2024;28:249–255. [CrossRef]
[35] Hay JE. Calculation of monthly mean solar radiation for horizontal and inclined surfaces. Solar Energy 1979;23:301–307. [CrossRef]
[36] Klucher TM. Evaluation of models to predict insolation on tilted surfaces. Solar Energy 1979;23:111–114. [CrossRef]
[37] Skartveit A, Olseth JA. Modelling slope irradiance at high latitudes. Solar Energy 1986;36:333–344. [CrossRef]
[38] Temps RC, Coulson KL. Solar radiation incident upon slopes of different orientations. Solar Energy 1977;19:179–184. [CrossRef]
[39] Matagne E, El Bachtiri R. Exact analytical expression of the hemispherical irradiance on a sloped plane from the Perez sky. Solar Energy 2014;99:267–271. [CrossRef]
[40] Myers DR. Solar radiation resource assessment for renewable energy conversion. Golden (CO): National Renewable Energy Lab (NREL); 2012. [CrossRef]
[41] Perez R, Ineichen P, Seals R, Michalsky J, Stewart R. Modeling daylight availability and irradiance components from direct and global irradiance. Solar Energy 1990;44:271–289. [CrossRef]
[42] Perez R, Stewart R, Seals R, Guertin T. The development and verification of the Perez diffuse radiation model. Albuquerque (NM): Sandia National Lab (SNL-NM); 1988. [CrossRef]
[43] Perez R, Seals R, Ineichen P, Stewart R, Menicucci D. A new simplified version of the Perez diffuse irradiance model for tilted surfaces. Solar Energy 1987;39:221–231. [CrossRef]
[44] Perez R, Stewart R, Arbogast C, Seals R, Scott J. An anisotropic hourly diffuse radiation model for sloping surfaces: description, performance validation, site dependency evaluation. Solar Energy 1986;36:481–497. [CrossRef]
[45] Khoo YS, Nobre AM, Malhotra R, Yang D, Rüther R, Reindl T, et al. Optimal orientation and tilt angle for maximizing in-plane solar irradiation for PV applications in Singapore. IEEE J Photovoltaics 2013;4:647–653. [CrossRef]
[46] Zomer C, Nobre A, Cassatella P, Reindl T, Rüther R. The balance between aesthetics and performance in building-integrated photovoltaics in the tropics. Prog Photovoltaics Res Appl 2014;22:744–756. [CrossRef]
[47] Da Silva MK, Narvaez DI, de Melo KB, Costa TS, de Siqueira TG, Villalva MG. Comparative analysis of meteorological databases and transposition models applied to photovoltaic systems. 1.